Pramāṇa, Vol. 14, No. 5, May 1980, pp. 349-362. © Printed in India.

An automated high precision calorimeter for the temperature range 200 K–400 K. Part II. Design of temperature controllers

H HECK*, I S WILLIAMS**, E S R GOPAL† and S JYOTHI†

Research School of Physical Sciences, Australian National University, Canberra ACT 2600
*Electronics Section.
**Now with the Department of Defence, PSB, Russel, Canberra
†Department of Physics, Indian Institute of Science, Bangalore 560 012

MS received 19 January 1980; revised 21 March 1980

Abstract. The design and construction of precision temperature controllers, capable of tracking the temperature of the samples to within 1 mK for ramp heating rates from 0·05 to 10 K per hour, are discussed. A tutorial section on the evolution of the control loop configuration is first given. This is followed by an outline of the refinements of the basic control loop desirable in the actual implementation of the electronic controller. The novel features of the present system and its performance are then briefly discussed. Finally the inadequacy of the conventional PID controllers for this application, the estimation of the time constants of the physical system needed in the design of the electronic controllers and the pitfalls in using a simple model of the heater plus thermometer assembly with a single pole are also discussed.

Keywords. Temperature controller; linear system; PID controller; high precision calorimeter; control loop configuration.

1. Introduction

Precise control of temperature has been an important problem of process control in many areas of science and technology. In adiabatic calorimetry, especially of the precision type described in an earlier paper (Williams *et al* 1978, hereafter referred to as Part I), the temperature control problems become very severe. In the vacuum adiabatic calorimeter the temperature of the sample may vary at different rates and yet the surrounding environment must follow the sample temperature to within a millidegree C.

Because of the widespread need for temperature controllers, a large amount of literature exists on the topic (Griffith 1951; Coxon 1960; Miles 1965; Kutz 1968; Roots 1969; Stoecker 1971). However all these texts were written purely from the point of view of either heuristics or of the feedback control system theory. The same is true of the numerous papers on the subject. As a result, systematic ways of designing the control unit with the required gain, time constants and other characteristics do not seem to have received adequate attention, especially for laboratory-type physico-chemical applications.

The present paper is therefore divided into sections of which §§ 2 and 3 are brief and tutorial in nature. Some of the novel features of the present control system are discussed later, followed by a brief discussion of the performance of the system.

The results of the physical investigations performed with the apparatus are reported separately (Part I; Williams *et al* 1979, 1980).

2. Statement of the control problem

A simple ON-OFF controller has inescapable overshoots and undershoots of temperature about the mean value. A better constancy of temperature is obtained with a proportional controller, wherein power $\dot{Q}$ proportional to the difference between the instantaneous temperature T and the desired set temperature T_s is applied to the system. The quiescent loss of heat from the system is proportional to $(T-T_a)$, where T_a is the ambient temperature. Thus for a system of thermal capacity MC, the heat balance is of the form

$$\dot{Q}=MC(dT/dt)=P(T-T_s) - L(T - T_a) + A_0, \tag{1}$$

where P is the proportionality constant of the controller power output and L that for the heat loss from the system. A_0 is the mean off-set output of the controller, equal to $L(T_s-T_a)$ when the error input $(T-T_s)$ has become zero. This ideal system approaches the set temperature T_s exponentially and there is no overshoot or undershoot. Apart from the serious problems caused by the non-ideal time-lag between the sensing of the temperature and the correcting heat input, which will be discussed below, the simple proportional controller has another disadvantage for physicochemical investigations. If a new set temperature T_s' is needed, the controller will settle into a finite error signal $P(T_s-T_s')$. So the absolute independent temperature calibration of the temperature sensor would no longer be valid. This off-set error can be reduced by increasing the controller gain P, but this would inevitably lead to oscillations because of the time-lag between the temperature sensing and the control power output (Caldwell *et al* 1959). Another way to solve the problem would be to introduce a control power proportional to the integral $\int (T-T_s)dt$ of the error signal. When this complexity is attempted, it is not too much of a bother to solve the sluggish response of the ordinary proportional controller by introducing a derivative term $(d/dt)\ (T-T_s)$ so that the system can follow rapid changes of temperature. Thus one has

$$\dot{Q}=MC(d\tau/dt)=I\int \tau dt+P\tau+D\,\frac{d\tau}{dt}-L+A_0, \tag{2}$$

where $\tau=T-T_s$ is the temperature deviation from the set value and the loss function L can be more general than a mere proportionality upon $(T-T_a)$. This is the canonical form of the PID controller of the linear system control theory and the PID controller is usually considered to be the most refined and versatile of linear controllers. The working of PID controllers is explained in a very simple manner by Warren (1967).

Being a second-order differential equation, the solutions may result in undamped oscillations if the gains P, I, D are not adjusted properly. Further the possibility of instabilities arising from the lags in temperature sensing will have to be countered

by appropriate lead-lag networks. Systematic ways of dealing with these questions in a practical laboratory situation do not seem to be well-known. Therefore § 3 deals with this question in a simple tutorial fashion. If temperature controls at millidegree levels are attempted, the task of sensing temperatures at these levels and the design of adequately sensitive and stable electronic circuitry become nontrivial problems.

3. Design of basic control system for linearly varying temperatures

The sample in the adiabatic calorimeter is usually heated at a steady rate and to a first approximation one can say that the shields should follow or track a steady rise of temperature. It is known (D'Azzo and Houpis 1966) that a simple proportional controller, with a transfer function $G(s)=K_0$, would give an off-set error for a general steady temperature and that the off-set can be eliminated by the addition of an integrator. Thus a type-1 system with a dominant transfer function $G(s)=K_1/s$ would give zero off-set for any steady temperature but would give an off-set for a linearly varying temperature. A type-2 control system with the dominant transfer function $G(s)=K_2/s^2$ is the simplest controller which will follow a ramp input with zero off-set error and therefore it forms the start of our discussions.

The simplest equivalent network of a heater is a parallel combination of a resistance R_H and a capacitance C_H with a time constant $\tau_H=R_H C_H$ (figure 1a) so that its transfer function is of the form $K'/[s+(1/\tau_H)]$ (Roots 1966). As will be discussed in appendix I, τ_H is of the order of 10^2 sec. There is a similar model for the thermometer or temperature sensor with a time constant of the order of 10^1 sec. In our apparatus the heater is wound on the adiabatic shield on which the thermometer is also fixed and the control is effected from outside. The situation would be similar in most other applications. The effect of the energy put into the heater is sensed by the thermometer to actuate the control system. So the transfer function for the heater-thermometer block may be taken as $1/(s+A)\ (s+B)$, where $A^{-1}=\tau_{\text{heater}}\approx 10^2 s$, and $B^{-1}=\tau_{\text{thermometer}}\approx 10^1 s$ (figure 1b). It must be mentioned that some workers have used a simple one-pole network $1/(s+A)$ for the heater + thermal sensor combination. However this can lead to instability under some conditions, as will be discussed in appendix II.

The combination of a type-2 controller with a heater + temperature sensor gives a control network as shown in Figure 2a. In order to study the stability of this network it is convenient to use the root locus method. The open loop transfer function is

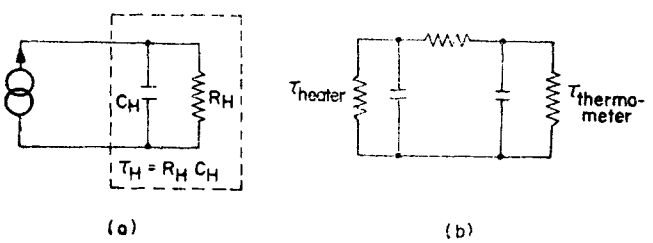

Figure 1. (a) Equivalent circuit of a simple heater. (b) Equivalent circuit of the heater plus thermometer assembly.

$G(s) = K/s^2(s+A)\ (s+B)$. The characteristic equation is $s^2(s+A)\ (s+B)+K=0$. Using the simple methods of finding the main features of the root locus plots (Dransfield 1968; Baeck 1968) one easily obtains the following simple features: (i) There are four branch loci, as there are 4 roots of the characteristic equation. (ii) The loci start for $K=0$ at $0, 0, -A, -B$ (poles of $G(s)$) and end at infinity (the zeros of G) for $K \to \infty$. (iii) From the number of finite poles and zeros, the angles made by the asymptotes with the X-axis (Rl σ-axis) are obtained as $\pm 45°$ and $\pm 135°$. (iv) The point of intersection of the asymptotes with X-axis is $-(A+B)/4$. (v) On the real axis the loci lie between $-A$ and $-B$. (vi) A breakaway point exists at 0 and another one between $-A$ and $-B$. (vii) The loci do not cross the Y-axis (Im σ-axis). Based on these features one can get the general shape of the root locus plot to be as shown in figure 2b.

The full details of the root locus plot with numerical values could be drawn using a HP 9820 calculator and a XY plotter. Numerical methods also exist which would yield the same information about the precise shape of the root locus plot. The presence of the branches to the right of the imaginary axis (real part of the root σ being positive) immediately shows that the system is unstable and that this is so for all values of the gain K. This arises from the time constants (poles) of the problem in the type-2 controller.

Clearly the system should be stabilised before going further, i.e. compensators have to be added to the system. These lead lag devices can be used either in the forward feed or feedback loop of the system to provide the necessary change in the systems transfer function. In the calorimeter, the temperature differences are measured with thermocouples. Since the error signal alone is available for control, the conventional feedback compensation cannot be used and one has to apply cascade corrections. Also since the summing point is a very low impedance point, a thermocouple, it is not good to incorporate correction networks at the input. Instead one may follow the procedure of adding zeros to the system. Thus one may consider the control loop with the transfer function $G(s) = K(s+c)\ (s+d)/s^2\ (s+A)\ (s+B)$, formed by adding two zeros as shown in figure 3a. Assuming for simplicity the time constants to be such that $A<B<c<d$, one gets the main features of the root locus plot, such as the number of branches, the starting and ending points, locations on the axes and the locations of the asymptotes. The shape of the root locus plot, obtained by the methods outlined earlier, is shown in figure 3b. The system is still unstable. If the time constants are such that $A<c<d<B$ and further $(c+d)$

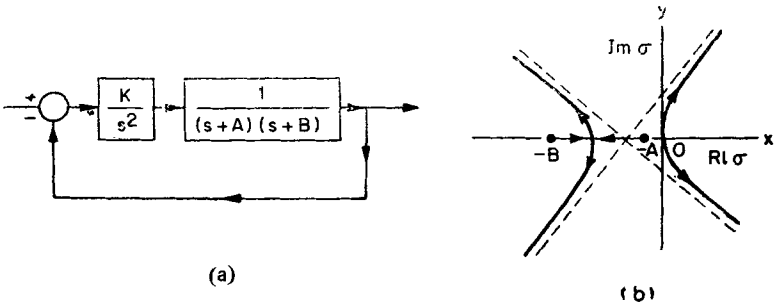

Figure 2. (a) Simple type-2 controller connected to a heater plus thermometer assembly. (b) Topological features of the root locus plot for the control system with $G(s) = K/s^2\ (s + A)\ (s + B)$.

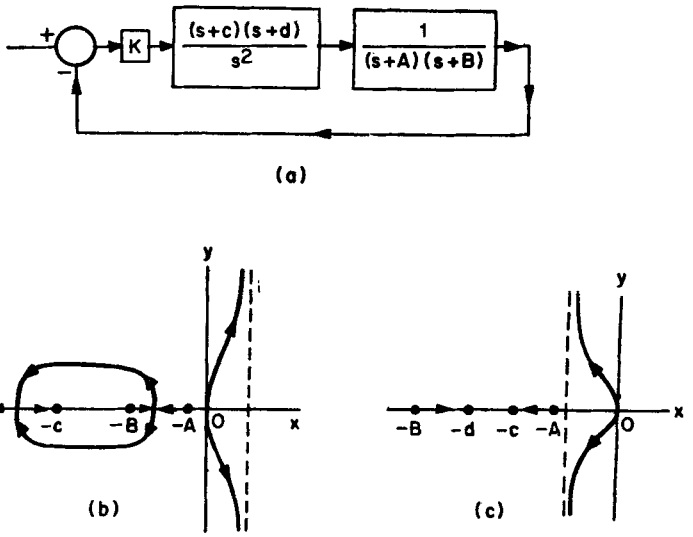

Figure 3. (a) Type-2 controller connected to a heater with two zeros added to the system. (b) Response of the system when the zeros are large. (c) Response of the system when the zeros are small compared to the poles.

$<(A+B)$, then the root locus plot has the shape shown in figure 3c. While the system is theoretically stable, the loci lie very close to the Im σ-axis (since $A^{-1} \approx 100\ s$). So there is low damping and hence very poor system response. Thus the network is not acceptable.

The solution to this problem is to pull the complex roots further away from the imaginary axis to give better system response. A simple way to effect this is to add a zero so that the transfer function is of the form $G(s) = K(s+c)(s+d)\,(s+e)/s^2(s+A)\,(s+B)$. For this system one may deduce the main features of the root locus plot as indicated above. The shape of the plot is shown in figure 4b for the case $A<B<c<d<e$. The system of figure 4a is clearly stable. If the time constants are such that

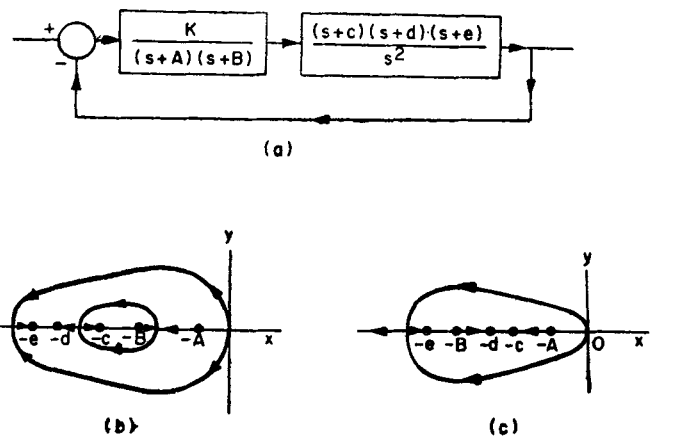

Figure 4. (a) Type-2 controller connected to a heater systems with three zeros added. (b) Shape of the root locus plot when the poles are smaller than the zeros. (c) Main features of the root locus plot when some of the zeros are small.

$A<c<d<B<e$, the features are slightly changed and the plot is shown in figure 4c. The system is still stable and acceptable.

Unfortunately those shown in figure 4 are not good solutions from the point of view of noise immunity in practice. In any electronic system the 50/60 Hz hum and their harmonics are always present. The pick-up of these signals from the wiring is not easy to avoid. Further the devices themselves produce noise at low levels. The differentiator Ks has a gain which increases with frequency and so would amplify the high frequency noise. The networks $(1+c/s)$ $(1+d/s)$ allow an unattenuated path for the high frequency noise, which then gets amplified by the $(s+e)$ differentiator block. It is for this reason of noise immunity that a straightforward differentiator is not preferred in control systems. It is only under some special conditions that a band limited rate amplifier is successful (Heck 1980).

To reduce the noise susceptibility, add an integrator and consider the control loop shown in figure 5a with $G(s)=K(s+c)\,(s+d)\,(s+e)/s^2\,(s+A)\,(s+B)\,(s+g)$. Let $A<c<d<B<e<g$, taking the clue from the considerations of figure 3c. One gets the qualitative features of the root locus plot to be as shown in figure 5b.

The time constants A^{-1} and B^{-1} are properties of the physical apparatus and the electronics engineer has little control over their values. For stability, the point of intersection of the asymptotes should be as far left to Y-axis as possible, i.e. $(A+B+g)$ must be much greater than $(c+d+e)$. With ordinary electronic components, it is not easy to get integration time constants much greater than say 1 second ($R=1M$, $C=1\mu F$ giving $RC=1$ sec). The extra freedom of making g as large as possible and keeping c, d, e small, consistent with an acceptable pass band for noise signals, makes the control loop of figure 5 a an acceptable one.

It must be mentioned that there are many other ways of analysing the control loops to arrive at the above or equivalent solutions of the problem. The present procedure seems to have the virtue of making the path and the solution quite transparent.

4. Improvements to the control system

In thermal systems, especially of the type discussed in part I, there is active heating

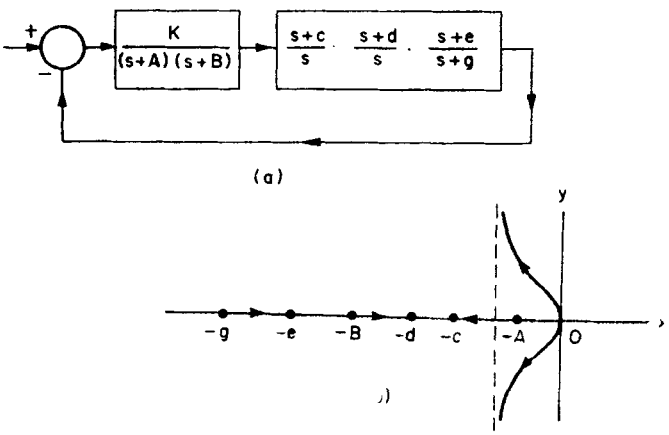

Figure 5. (a) Type-2 controller connected to a heater with zeros and lead/lag network added. (b) Topology of the root locus plot for $G(s) = K(s + c)(s + d)(s + e)/s^2(s + A)(s + B)(s + g)$.

with the help of heater windings operated by power amplifier outputs. There is however no active cooling. Though thermoelectric and other active cooling are possible it is more common to have passive cooling by radiation or conduction through the support tubes and structures. As discussed in appendix I the time constants of the two processes, about 10^2 s and 10^4 s, differ by orders of magnitude. To a first approximation one may take that the output power controller can heat but not cool the system. This requires a nonlinearity in the control loop so that, say, negative error signals activate the output power element but positive signals do not. Such a nonlinearity is easily provided by introducing a precision diode rectifier in the control path.

Secondly the control system assumes that the correcting power fed to the heater is proportional to the error input. In practice electronic amplifiers give an output voltage which is proportional to the input volatge and hence the output power fed to the heater is proportional to the square of the input error signal. This problem is solved by introducing a square-root amplifier in the electronic control loop. The circuit described by Smith (1972) is well suited for this purpose and has been used by us.

With these refinements the final circuit takes the form shown in figure 6. As is common in these studies, the basic control loop was tested by simulation on an analog computer. The transfer functions of the type $(s+d)/s$ and $(s+e)/(s+g)$, which are needed in the loop, could be realised in the hardware form by the simple circuits shown in figures 7a and 7b. However in order to ensure flexibility when testing the various units, the functions were actually realised using the circuits of figures 7c and 7d. While these circuits do increase the number of operational amplifiers somewhat, one has the great advantage of varying d, e, g without altering the gain of the system. Even in the final circuit of the electronic temperature controller it was found desirable to use these forms of the circuits (since the time constants of the physical system could be only approximately calculated and so one has to retain some flexibility in the time constants of the electronic controller). The control loop was found to be quite stable and efficient when tested by patching on the analog computer. Apart from stability one requires good response to step and other inputs and this was broadly optimum when the values were of the order of $(s+0{\cdot}1)/s$, $(s+0{\cdot}1)/s$, $(s+0{\cdot}1)/(s+1{\cdot}0)$. One could also check the instability when $(c+d+e)$ was made larger than $(A+B+g)$ as was observed in figure 5 b.

5. Circuit details

The central part of the final electronic controller circuit is shown in figure 8. Not shown are the details of the power supplies, overload indications and similar indi-

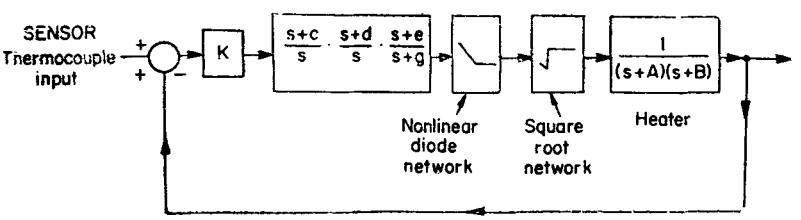

Figure 6. Final control loop incorporating nonlinearity and square root corrections.

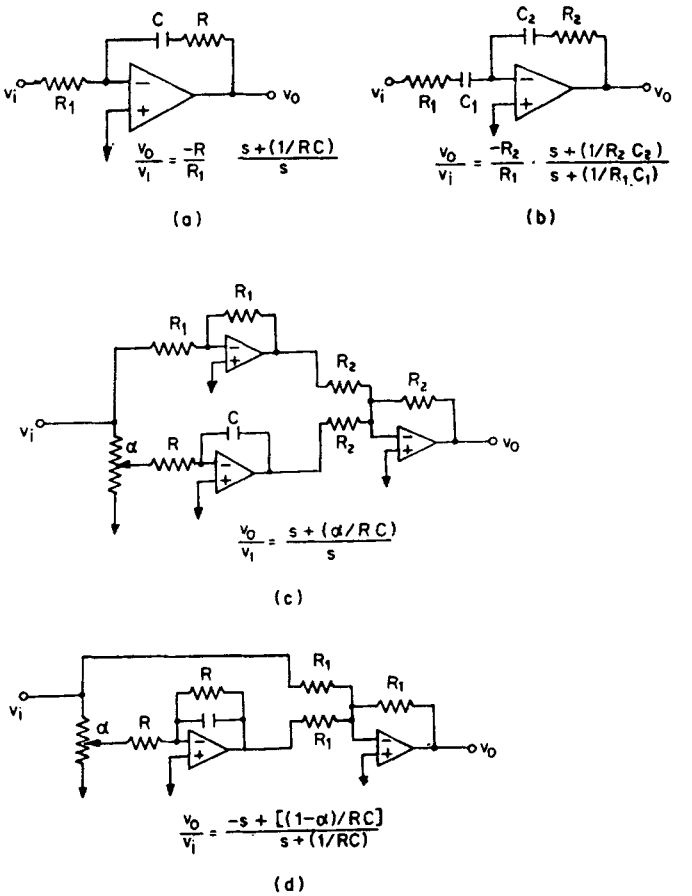

Figure 7. Hardware realisation of transfer functions. (a) Simple network for realising $(s + d)/s$. (b) Simple network for getting $(s + e)/(s + g)$. (c) Flexible form of network to obtain $(s + d)/s$. (d) Flexible network to get $(s + e)/(s + g)$ for $e \leq g$.

cative/protective devices incorporated into the final unit (Heck 1976, 1979). The complete drawings are available from one of the authors (H Heck).

In a system requiring control at millidegree levels of temperature, the noise levels and the d.c. stability at the input stages assume considerable significance. In the present calorimeter system, thermocouples (MacDonald 1978) were used to measure the temperature differences between the sample and the adiabatic shield, dictated by the small size of the thermocouple junction, the small time constant and the small heat conduction allowed through the fine thermocouple wires, thereby reducing the thermal link between the sample and the environment. However thermocouples have a thermo-emf of about 38 microvolt/deg and so voltages of the order of micro-or nano- volts are encountered at the input stages. These voltages were amplified with the help of a Keithley Model 148 nanovoltmeter. This instrument has a non-cumulative d.c. drift of less than 10 nanovolts per 24 hr, which is very critical in thermal measurements extending over 100 hr or more. The input noise level is less than 1 nanovolt peak-to-peak, which is also much better than what can be obtained in any simple manner. Indeed the stray noise in the calorimeter (pick-ups, hum, etc.) is

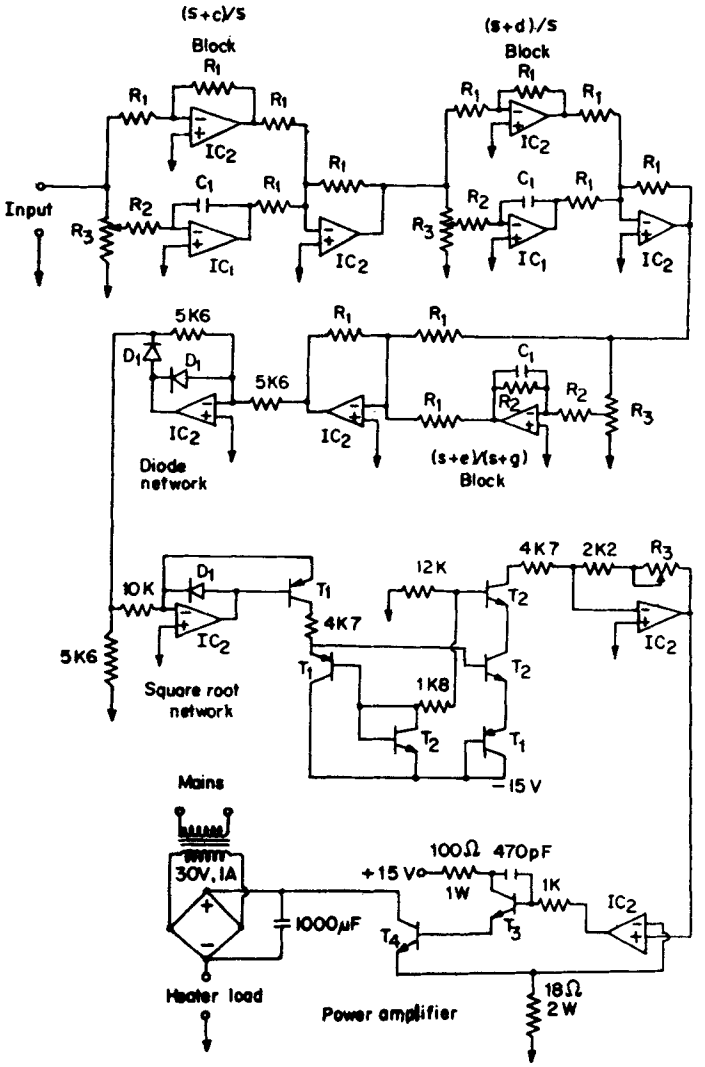

Figure 8. Circuit diagram of the electronic controller (R_1 = 10 K ohm, 1 %; R_2 = 1 M ohm, 1% R_3 = 10K potentiometer; C_1 = 1 μF; IC_1 = BB 3522; IC_2 = BB 3500; D_1 = AN 204; T_1 = 2N3906; T_2 = 2N3904; T_3 = 2N2102; T_4 = 2N3055).

very much higher than this and is of the order of microvolts. The nanovoltmeter used has a ±1 Volt output, which was used as the error signal to the input of the electronic controller shown in figure 8. The inputs to the nanovoltmeter have to be taken through special thermo-electric-free connectors and switches, because of the low level signals involved. The output of the nanovoltmeter is at a higher signal level and so ordinary precautions are adequate.

The circuit shown in figure 8 closely follows the control loop configuration of figure 6 and the various sub-units are easy to follow. The controller uses high quality operational amplifiers, dictated by the considerations of d.c. stability and noise performance. The need to use high stability components and low leakage capacitors in circuits involving long time constants is well-known. Since the controller has to operate for 100 hr or more in a routine fashion, attention to d.c. operating conditions

and to reliability considerations is very important. The final power amplifier has a floating mode. It is convenient in this particular application for trouble-shooting the cryostat in the early stages, since the different parts would be at different potentials. The heater windings have 25–100 ohms resistance and the controller has 25 W maximum power output. Under normal conditions power levels of only a few Watts are needed. The nanovoltmeter is operated in the 10–100 microvolt ranges (voltage gain 80–100 db). If the gain is set too high, then the noise signals inevitably present in the cryostat overload the electronic circuitry. If the gain is too low, the internal noise levels of the electronic controller begin to dominate over the operating signal degrading the temperature control. The gain of the amplifier influences the damping and the settling time of the controller, though a type-2 controller has zero-tracking error for all values of the gain.

The controller has been tested under various conditions. Figure 9 shows a mosaic of the error signal (output of the Keithley nanovoltmeter) recordings under different heating rates of the sample. The system stabilises within 3-5 cycles. The period of oscillations, $\sim$ 5·2 min., depends upon the *c*, *d*, *e* time constants. For heating rates from 0 05 to 10 K/hr the adiabatic shield could follow the temperature of the sample with rms fluctuations of the order of 1·2 mK.

There is no easy way to measure the tracking error if any in the system. A quantity of water was taken in a sealed sample holder and the melting point of ice was determined by monitoring the temperature of the shield. Assuming that the temperature at which the heating rate abruptly changed is an indication of the melting of ice, it was found that the difference in the apparent melting points at heating rates of 2·1 K/hr and 8·6 K/hr was $0{\cdot}7 \pm 1{\cdot}5$ mK. One must conclude that the tracking error if any is less than the measurement limits.

It may be mentioned in passing that conventional PID controllers tend to be type-1 controllers. They will have a finite tracking error when following a ramp input of temperature. This error can be made small by increasing the gain of the controller. The system noise would set a limit to the increase in gain. For the slow heating rates used in the present apparatus, it has been calculated that the tracking error could be made of the order of 1-2 mK, for the 80 db gain of the nanovoltmeter. The situation would become adverse when faster rates of heating are required. A type-2 controller clearly becomes necessary under such conditions.

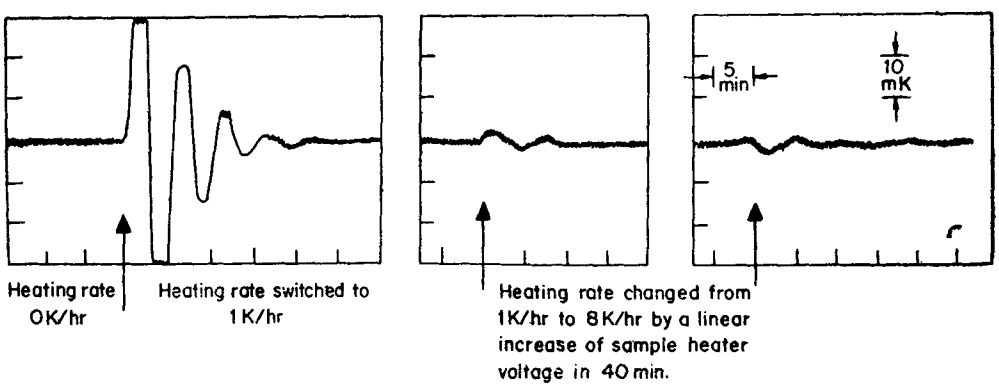

Figure 9. Mosaic of the controller performance. The thermocouple error signal, amplified by the nanovoltmeter, is given as a function of time for various heating conditions.

The response of the controller to very large error signals, driving it into the nonlinear region, has been satisfactory when sudden increases in the rates of heating are encountered. The controller rapidly follows the increase of temperature and settles down into control after a few oscillations. Such situations are often encountered in the beginning of the experiments when large differences of temperature are present before the controllers are put on. When the controller is driven into the nonlinear region by sudden decreases in the rates of heating, it latches up because of the absence of active cooling. The situation could possibly be improved by clamping the voltages across the integrator capacitors from becoming excessively negative. It would be necessary to ensure that the clamping diodes do not introduce leakage resistances in the reverse bias conditions, especially in circuits involving large time constants.

Finally a comment is necessary on the time constants of the system and the controller. As shown in the appendix I, the time constant of the heater wrapped on the adiabatic shield is calculated to be about 88 sec under active heating conditions. Under passive cooling conditions, the heat transfer is through radiation and through conduction along the support structures. The time constant for the passive cooling is estimated to be a few hours. These are the pieces of information used in the design of the electronic controller. Experimental measurements of the time constants using heating and cooling cycles give values which are within 50% of the calculated values. The time constants of the controller have sufficient lattitude in design to cover these variations. The method of analysis has obvious applications to other situations.

Appendix I: Estimation of the time constant of the heater

The calculation of the time constants of the adiabatic shield heater is made with the help of a sketch of the shield heater shown in figure 10. The copper adiabatic shield can, of dimensions ~ 5 cm diameter and ~ 15 cm length and of mass $M \sim 900$ grams, has the heater wrapped on it. The can is supported inside a vacuum enclosure and has aluminium foil wrapped round the heater to reduce radiation losses. Assuming the operation around 300 K, the specific heat of copper C_p is $\approx 0{\cdot}38$ J/g K and so the thermal capacity is $MC_p \approx 900 \times 0{\cdot}38 \approx 340$ J/K. Thus the effective thermal capacitance C_{th} can be taken as ~ 340 J K^{-1}.

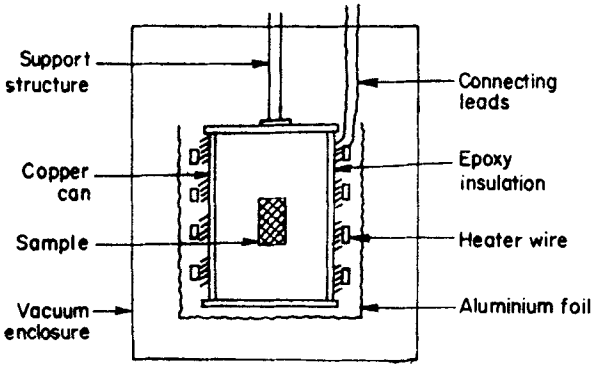

Figure 10. Sketch of the adiabatic can heater.

Consider now the active heating case. 20 turns of heater wire of effective diameter ~ 1 mm are wound bifilarly over the can and thermally bonded with epoxy resin. Thus the effective area of contact through which heat is transferred to the can is nearly 60 cm^2. The insulating epoxy resin may be taken to have an average thickness of $\sim$0·2 mm and its thermal conductivity as $\approx$1·3 mW/cm deg. For a 1°C temperature difference, the heat conducted would be 3·9 W and so one may take the thermal resistance of the heater to be $R_{th} \approx 0{\cdot}26$ K/W. Neglecting the heat capacity of the heater, the aluminium foil and the epoxy resin, the time constant of the active heater comes out to be $C_{th} \times R_{th} \approx 88$ sec.

In the passive cooling case, one notices that most of the heat loss from the can is to the surrounding floating vacuum chamber walls. The sample kept inside the adiabatic can is quite small and its area can be neglected. One has to estimate the heat transfer through the support structure and through radiation. The support structure consists of three stainless steel rods of ~ 2 mm diameter and ~ 7 cm length. Assuming the thermal conductivity to be 0·25 W/cm deg., the heat transported through them for a 1°C difference of temperature is nearly 3 mW. In addition there are a number of wires attached to the heater and other sensors placed on the adiabatic can. These may be taken to the equivalent of 6 copper wires of 0·5 mm diameter. The thermal conductivity of copper being 3·9 W/cm deg., the heat transferred through the copper wires for a 1° temperature difference is nearly 7 mW. The total area of the can is 250 cm^2 and because of the aluminium foil the emissivity can be taken as 0·05. Thus for a 1° temperature difference compared to the outside, the heat radiated would be $\sim$ 8 mW. Thus the total heat transfer by passive cooling is $\sim$ 18 mW/deg. and so $R_{th} \approx 55$ K/W. Consequently the time constant for the passive cooling mode is $\approx 340 \times 55 \approx 18{,}000$ sec. Such long time constants are not uncommon in adiabatic systems where thermal isolation from the surroundings is essential.

The experimental measurement of the time constants is done after assembling the cryostat, when all the required temperature sensors are in position. A step heating is given to the heater winding and the temperature rise is monitored. The approximately exponential temperature rise gave a time constant of nearly 62 sec for the heating case, in approximate agreement with the calculated value. After heating the adiabatic can to a temperature of ~ 2°C above the surrounding the passive cooling is monitored. The passive cooling time constant is obtained as ~ 2 hr. The probable source of the somewhat large difference from the calculated values is the presence of the connecting wires with vacuum grease, varnish and other components which are not taken into account in this idealised consideration. As long as the passive cooling time constant is much larger than the active heating time constant, one has no problem in the actual control system, where the passive cooling time is taken to be infinitely large compared to the active heating situation. Also the design of the electronic controller has sufficient freedom to take into account the rather large uncertainties in the estimation of the time constants.

Appendix 2: Consideration of a single pole network model for the heater plus thermometer combination

In many cases of thermal control, a simple network $1/(s+A)$ has been used to represent the heater plus thermometer combination. The final controller performs ade-

quately in many cases. In this appendix we present some of our results which show the regions where the control was adequate and where it failed.

Suppose one considers a type-2 controller connected to a one pole network, giving $G(s)=K/s^2(s+A)$. Using the methods of finding the main features of the root locus plots, one can easily obtain the shape of the root locus plot to be as shown in figure 11, giving a clear instability. This is so for all values of the gain K and thus one must stabilise the system first. As was done with figure 3a, the starting point is to add zeros making a transfer function $G(s)=K(s+C)(s+D)/s^2(s+A)$. Assuming the time constants to be such that $A<C<D$, one obtains the topological shape of the root locus plot to be as shown in figure 12. The system is stable and could form the basis for building a controller.

Indeed similar considerations were the basis for an electronic controller built earlier. The controller worked well when the calorimeter was assembled initially in air but became unstable when the calorimeter was evacuated. In studying the oscillations and the response to pulses of heating and cooling in vacuum, the probable reason for the instability became evident. The heater plus thermometer combination should really be considered as a two-pole network instead of the one-pole approximation.

In other words, while the controller is built on the analysis of the network $G(s)=K(s+C)(s+D)/s^2(s+A)$, the calorimeter is really described by a transfer function $G'(s)=K'(s+C)(s+D)/s^2(s+A)(s+B)$. The behaviour of G' has already been discussed. If the time constants are such that $A<C<D<B$ and $(C+D)<(A+B)$, the system is stable (figure 3c). If however A and B become small and $C+D$ become greater than $A+B$, the point of intersection of the asymptotes moves to the right of

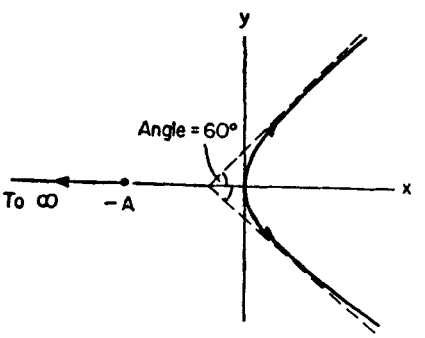

Figure 11. Shape of the root locus plot for a system with the transfer functions $G(s) = K/s^2(s + A)$.

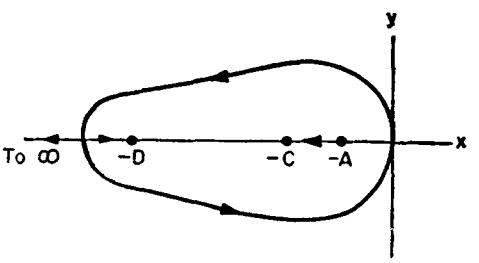

Figure 12. Approximate root locus plot for a type-2 control system with a transfer function $G(s) = K(s + C)(s + D)/s^2(s + A)$.

the Y-axis resulting in unstable conditions. When the calorimeter is assembled in air, the heat exchange between it and the surrounding is efficient. The time constants A^{-1} and B^{-1} remain small and one has the case of figure 3c. When the calorimeter is evacuated the heat exchange is reduced and the time constants become large. A and B become small and the root locus moves to the right of the Y-axis. At this stage the system becomes unstable.

This illustration of the earlier electronic controller, which was satisfactory under some conditions but became unstable under other operating conditions, shows the need to make detailed studies of the stability of the control loop before constructing a precision temperature controller.

References

Baeck S H 1968 *Practical servomechanism design* (New York: McGraw-Hill) Ch. 6
Caldwell W I, Coon G A and Zoos L M 1959 *Frequency response for process control* (New York: McGraw-Hill) Ch. 3
Coxon W F 1960 *Temperature measurement and control* (London: Heywood)
D'Azzo J J and Houpis C H 1966 *Feedback control system analysis and synthesis* (New York: McGraw Hill) p. 177
Dransfield P 1968 *Engineering systems and automatic control* (New York: Prentice Hall) Ch. 7
Griffith R 1951 *Thermostats and temperature regulating instruments* (London: Griffin)
Heck H 1976, 1979 Report on the adiabatic calorimeter temperature controller R. S. Phys. S., Aust Natl. Univ. (unpublished reports)
Heck H 1980 (to be published)
Kutz M 1968 *Temperature control* (New York: Academic Press)
MacDonald N H 1978 *Control instrum.* **10** 31
Miles V C 1965 *Thermostatic control* (London: Newnes)
Roots W K 1969 *Fundamentals of temperature control* (New York: Academic Press)
Smith D T 1972 *J. Phys.* **E5** 528
Stoecker W F 1971 *Design of thermal systems* (New York: McGraw-Hill)
Warren J E 1967 *Control instruments mechanisms* (England: W. Fouesham). Ch. 6, 7 and 8
Williams I S, Street R and Gopal E S R 1978 *Pramana* **11** 519
Williams I S, Gopal E S R and Street R 1979 *J. Phys.* **F9** 431
Williams I S, Gopal E S R and Street R 1980 (to be published)